Askandar and Mahmood
Int J Concr Struct Mater (2020) 14:7
https://doi.org/10.1186/s40069-019-0386-4

International Journal of Concrete Structures and Materials

RESEARCH Open Access

Torsional Strengthening of RC Beams with Continuous Spiral Near-Surface Mounted Steel Wire Rope

Nasih Habeeb Askandar[1,2*] and Abdulkareem Darweesh Mahmood[2]

Abstract

The strength of reinforced concrete members can be enhanced using externally bonded reinforcement (EBR) and near surface mounted (NSM) methods. However, small number of studies has adopted the NSM method for torsional strengthening. To date, no study has examined the use of spiral NSM steel wire rope and epoxy adhesives for torsional strengthening. Therefore, this study examines the behaviour of RC beams subjected to the combined actions of torsion and bending moment when they are strengthened with spiral NSM steel wire rope (Ø8 mm) in different configurations. For this purpose, six beams of 15 cm × 25 cm × 200 cm were casted. One of these beams was conventional, whereas all the other beams were strengthened with spiral NSM steel wire rope. During the testing process, the twist angle at the torque intervals, first cracking torque, ultimate torque and ultimate twist angle of the conventional beam were compared with those of the strengthened beams. The torsional performance of the RC beams was significantly improved using spiral NSM steel wire rope in various spiral NSM configurations.

Keywords: reinforced concrete beam, torsional behaviour, strengthening, near surface mounted, spiral, steel wire rope

1 Introduction

Apart from the flexure and shear resistances of reinforced concrete (RC) structural elements, torsion resistance is also a crucial factor that must be considered for peripheral beams in multi-storeyed buildings, ring beams at the base of circular tanks, edge beams of shell roofs and beams supporting overhang slabs and helical staircases. The torsional capacity of these members needs to be maximised due to several factors, including structural damage, deterioration and increased loading.

Strengthening materials can be applied in two ways to reinforced concrete (RC) structures: (1) externally bonded reinforcement (EBR) method, where the strengthening materials are applied externally to the concrete surface; and (2) near surface mounted (NSM) method, where the strengthening materials are incorporated into the concrete cover in pre-cut grooves (ACI 440.2R-08 2008).

The NSM strengthening technique, considered an accurate alternative to the EBR technique, involves cutting grooves in a beam specimen's concrete cover and then inserting and embedding strengthening materials into the grooves using an adhesive. The NSM technique provides other advantages over the EBR technique, including higher productivity of bonding and better protection. The NSM technique can also address the limitation of the EBR method in its peak strain, which due to premature debonding is below the ultimate strain. The great confinement granted of the adhesive and the surrounding concrete is considered to be the best benefit of the NSM technique (De Lorenzis and Teng 2007), which prevents debonding. This strengthening method has

*Correspondence: nasih.askandar@spu.edu.iq
[1] Halabja Technical College of Applied Sciences, Sulaimani Polytechnic University, Sulaymaniyah, Iraq
Full list of author information is available at the end of the article
Journal information: ISSN 1976-0485 / eISSN 2234-1315

already been shown to be reliable for the shear, flexural and both shear and flexural strengthening of RC beams. Instead of FRP materials, many research studies have also used steel wire ropes for flexural and shear strengthening by the NSM method, and column confinement. There were also a few studies using internal spiral stirrup instead of vertical. On the other hand, application of crossed inclined, NSM or EBR (diagonal or X-type steel reinforcement or FRP ropes) in deficient RC structural members for strengthening or increasing their torsional or/and shear capacity is another way that utilized for torsional or shear strengthening, that has been internally or externally applied, as shown in Table 1.

Nevertheless, only a few previous researches (Al-Bayati et al. 2016, 2018; Askandar and Mahmood 2019) investigated the use of the NSM technique in torsion strengthening. For example, (Al-Bayati et al. 2016) tested 10 samples of beams: two beams were used as controls, and the other eight beams were strengthened using CFRP laminates to their four sides. CFRP laminates were inserted into grooves using the NSM method. An adhesive epoxy was used in four strengthened beams, and a modified cement-based adhesive was applied as an alternative for epoxy in the four other beams. (Al-Bayati et al. 2018), applied the same torsion strengthening technique, but they tied a CFRP rope around the beam cross section with an equivalent CFRP percentage instead of applying CFRP laminates to the all sides of the beam. They used a cement-based adhesive in their experiment and tested four beams, namely, two similar control beams and two additional beams with torsion strengthened using a CFRP rope and epoxy. They applied the same strengthening technique for the two strengthened beams to verify the accuracy of their findings. (Askandar and Mahmood 2019), examined four beams: one beam was used as control, and the other three beams were strengthened by inserting a 2-U shaped welded steel bars into grooves by using the NSM method. An adhesive epoxy was used in all strengthened beams.

Many studies have applied the NSM strengthening method to improve RC beams ' flexural and shear strength. Nevertheless, only few of these studies have concentrated on torsion strengthening (Al-Bayati et al. 2016, 2018; Askandar and Mahmood 2019), and the use of spiral steel wire rope for torsion strengthening of RC beams has not been studied previously. In order to fill this gap, this study explores the characteristics of RC beams subjected to the combined actions of torsion and bending moment when they are strengthened by spiral NSM steel wire rope in different configurations.

2 Experimental Study

2.1 Torsion Strengthening Configurations

Six rectangular RC beams with 250 mm depth, 150 mm width and 2000 mm length were cast using ready-mixed concrete. The beams were designed intentionally to display torsion failure at beams' central part. The length of the central part was set to 1.0 m to allow for the formation of single spiral crack at the angle of 45° within the full length of the test region part of the beams. Figure 1 illustrates the steel reinforcement details and the cross-section dimensions of the beams. Accordance to the (ACI 318 M-14 2014), all beams were under-reinforced to simulate torsion-deficient beams under possible loading condition. The minimum spacing of the transverse reinforcement was also intentionally exceeded allow the observation of torsional failure and prevent the stirrup from restricting the torsional cracks. The groove details for all five strengthened beams are shown in Fig. 2. Grooves with a width of 20 mm and a depth of 20 mm are

Table 1 NSM strengthening technique literature background.

Strengthening field	Literature background
Shear	(Mofidi et al. 2015; Ramezanpour et al. 2018; Almassri 2015; Rahal and Rumaih 2011; Kammona and Al-Issawi 2018; Hayder Hussain and Al-Issawi 2018; De Lorenzis and Nanni 2001; Breveglieri et al. 2014; Chalioris et al. 2018)
Flexural	(Zhang et al. 2017; Wu et al. 2013; Kishi et al. 2005; Hosen et al. 2014, 2016, 2017; Gopinath et al. 2016; Ghanim and Al-Abbas 2018; Franco et al. 2018; El-Hacha and Gaafar 2011; El-Gamal et al. 2014; Almusallam et al. 2013; Al-Mahmoud et al. 2010; Shukri et al. 2016; Sharaky et al. 2014; Hong et al. 2018; Noroozieh and Mansouri 2019; Seo et al. 2016; Kaya et al. 2016)
Shear and flexural	(Sharaky et al. 2017; Barros et al. 2005)
Steel wire ropes	(Yang et al. 2009; Li et al. 2018; Kim et al. 2007; Haryanto et al. 2018)
Column confinement	(Wei et al. 2018; Wei and Wu 2014)
Internal spiral stirrup	(Shatarat et al. 2016; Saha and Meesaraganda 2019; Karayannis and Chalioris 2013; Karayannis et al. 2005; Chalioris and Karayannis 2013; Hindi and Browning 2011)
Crossed inclined, diagonal or X-type steel reinforcement or FRP ropes	(Tiwary and Mohan 2015; Chalioris and Bantilas 2017; Chalioris et al. 2008)

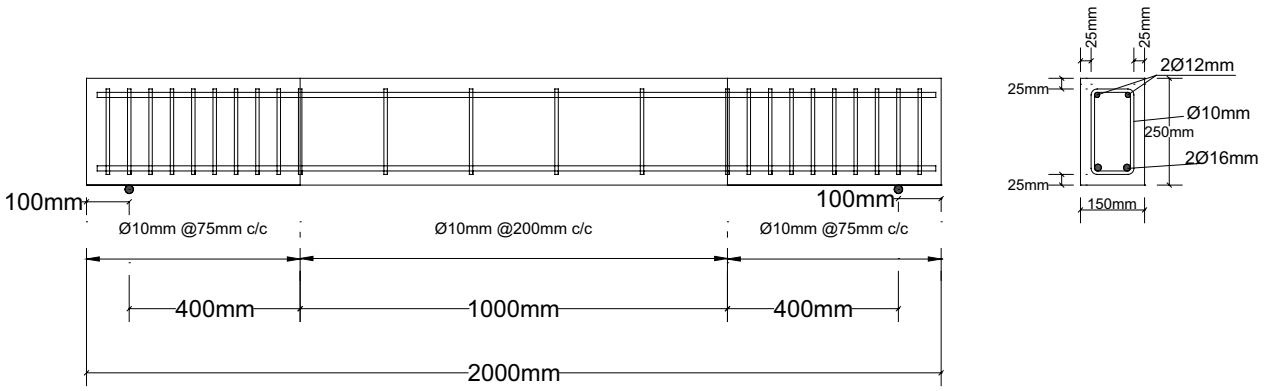

Fig. 1 Dimensions and reinforcement details of the test beams.

cut in the concrete beam cover area of 25 mm, and steel wire rope (Ø8 mm) was embedded in these grooves. For these beams, the c/c perpendicular spacing's of grooves were set to 113, 141, 188, 283 and 566 mm.

2.2 Material Properties

For all six beams, ready-mixed concrete was used. The supplied concrete's compressive strength ($f'c$) was evaluated after 28 days. In calculating the compressive strength, the average results of three concrete cylinders (100 mm in diameter and 200 mm in height) on the day of the test were considered. Sikadur-30P epoxy was used as an adhesive to fill the grooves of the strengthened beams.

Three bars with the same diameters and three pieces of steel wire rope (Ø8 mm) were subjected to uniaxial tensile tests to determine their yield and ultimate strength (f_y, f_u) as recommended by (ASTM A370-10 2010).

Table 2 summarises the mechanical properties of the concrete, stirrup steel bar, steel wire rope, the average compressive strength of the concrete ($f'c$) and the average test results for the steel bars. Table 3 shows the epoxy's properties depending on the specifications supplied by the manufacturer.

2.3 Specimen Preparation

After 28 days of curing, grooves were cut into the concrete cover of the specimens to install the strengthening steel wire rope. These grooves were cut in the spiral direction around the beam cross section, angle of spiral inclination Ø was 45° and dimensions were greater than 1.5 db × 1.5 db (ACI 440.2R-08 2008) (where db refers to the NSM steel wire rope reinforcement diameter). For cutting, a special concrete saw (Handle Grinder) was used with a diamond cutting saw blade. A hammer drill and chisel were used to remove the remaining concrete lugs and roughen the grooves' deeper surface. As shown in Fig. 3, these grooves were then smoothed and cleaned with a wire brush and a high-pressure air jet. As shown in Fig. 4, the strengthened steel wire rope was inserted into the spiral grooves by fixing in one end with the aid of anchor fix and stretching in the other end with the aid of small stretcher tool. These grooves were then filled around the steel wire rope with epoxy adhesive groove filler (Sikadur-30LP) and the surface was levelled as shown in Fig. 5. The beams were stored for 2 weeks to maintain the full strength of the epoxy.

2.4 Test Setup and Instrumentation

The rig of the test is shown in Fig. 6. A 200-ton hydraulic jack on the active support was used to transfer the load. The load had a lever arm of 500 mm from the vertical beam axis. To measure the load applied periodically, a compression load cell with a capacity of 100 tons was used. The hydraulic jack had a moving length of 250 mm and the beams were lengthened longitudinally after cracking. To prevent any lateral constraints and avoid any resulting compression, the beams were allowed to move freely by supporting the ends of the beams on the rollers at the un-resistance support. The angle of twist of the free end (the point of application of the torque) was determined using a dial gauge at that point with the aid of the downward length of the lever arm.

The loading frame in the laboratory of the civil engineering department was used to apply the load on the beam samples. A proper support condition was arranged to allow rotation about the longitudinal beam axis and the lever arms were attached to the specimen to provide a torsional moment, as shown in Fig. 6. When the position of the lever arm happens to coincide with the support, the beam was constantly subjected to pure torsion. The lever arm was kept beyond the two supports in order to apply simultaneous bending and torsion.

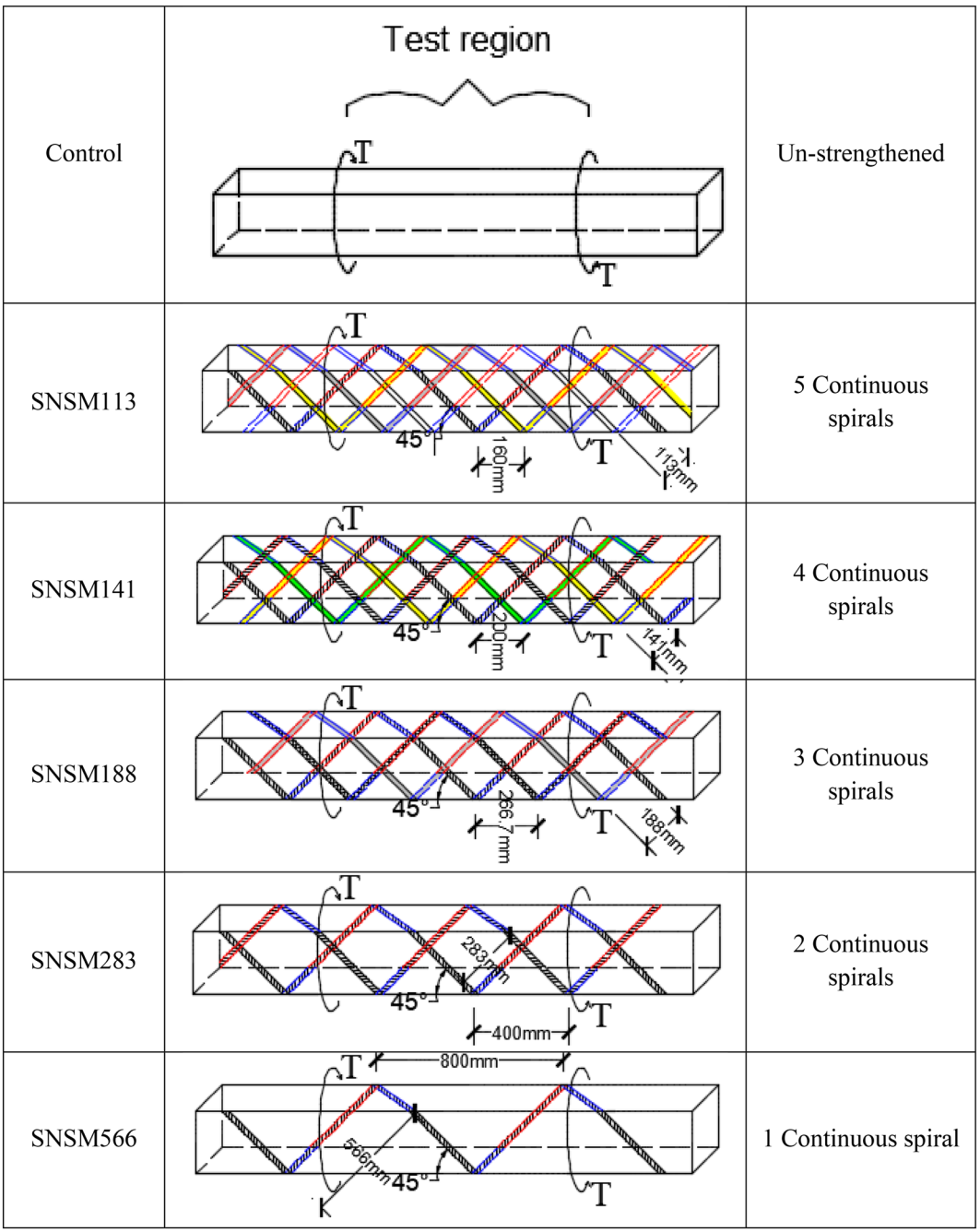

Fig. 2 Strengthening of the test beams.

Table 2 Mechanical property of the concrete, stirrup steel bar and steel wire rope.

Material	Compressive strength (MPa)	Yielding tensile strength (MPa)	Ultimate tensile strength (MPa)
Concrete	48	–	–
Steel bars of Ø10 mm	–	541	666
Steel wire rope of Ø8 mm	–	–	702

Table 3 Sikadur®-30 LP (two-part epoxy impregnation resin).

Appearance and colours	Part A: white; Part B: black; Parts A + B: light grey
Density (at 23 °C)	~ 1.65 kg/lt (parts A + B)
Mixing ratio	Part A:B = 3:1 by weight or volume
Layer thickness	30 mm max
Open time	90 min (at + 25 °C)
Viscosity	Pasty, not flowable
Service temperature	− 40 °C to 45 °C (when cured at > 23 °C)
Tensile strength	15 MPa to 18 MPa (when cured for 7 days at 23 °C)
Shear strength	17 MPa to 21 MPa [40 °C to 55 °C (7 days)]

- Three dial gauges were used: two of them were used to compute the displacements under the lever arm, and the other one was placed at the centre for the central displacement measurement.
- A distance of 400 mm between the support centre and the lever arm was maintained in order to bend along with torsion.
- The hydraulic jack load was transferred to the sample using the spreader beam at the end of the lever arm connected to the specimen. In this case, at the end of each lever arm, half of the load was applied.
- The overall length of the beams was 2.0 m; out of all, the beam's part between the supports had a length of 1.8 m and a projection of 0.1 m outside the support. The central part of the specimens of 1.0 m length was subjected to a combination of flexural and torsional moments, while the other parts of the beams that lie between the end supports and lever arms were under combined bending and shear forces. The torque in the middle test region part of the beams was calculated by multiplying the half of the total applied load by the length of the lever arm, and the twist angle was calculated as the sum of the twist angles from the both lever arms.

2.5 Test Procedure

The hydraulic testing machine in the civil engineering laboratory was used to test the beam samples, as shown in Fig. 7. The supports should be twisted and the applied load should be transferred to the two points that express the moment arm from the centre of the machine. Figures 6 and 7 show the loading frame used in this experiment, which was consisted of an I-section (200 mm × 80 mm × 8 mm)

Fig. 3 Continuous spiral NSN groove preparation.

Fig. 4 Continuous spiral NSN steel wire rope installation.

fastened to dual steel channels (100 mm × 50 mm × 8 mm). These steel channels were tied from the bottom by strong bolts after being placed around the beam cross-section. Concerning the longitudinal beam axis, the lever arms provided the required 500 mm eccentricity. As shown in Fig. 6, The 200 mm depth and 2 m length I-section steel spreader beam was used to transfer the loads from the centre of the machine to the two lever arms. Using the recorded videos and load increments from the data logger, increment readings from the dial gauges were recorded at each loading while the cracks were recorded when they occurred.

2.6 NSM Steel Reinforcement Ratio

The continuous spiral NSM steel wire rope reinforcement ratios for the strengthened specimens are shown in Table 4. The volumetric ratios of continuous spiral NSM steel wire rope reinforcement, ρ_{snsm}, were calculated using Eq. 1 (Chalioris and Karayannis 2013).

$$\rho_{\text{snsm}} = \frac{\text{volume of steel wire rope in one pitch}}{\text{Volume of concrete in one pich}} = \frac{A_{ss}P_{ss}}{A_c S_{SNSM} sin\theta} \quad (1)$$

2.7 Twist Angle Measurements

The twist angle was measured using a dial gauge that was connected to the lever arms' bottom at a point of 500 mm from the centre of the beam longitudinal axis. This dial gauge recorded the lever arm's downward value to quantify the twist angle in radians.

3 Results and Discussion

The values of cracking torque (T_{cr}), ultimate torque (T_u) and ultimate twist angle (θ_u) of the concrete beams are listed in Table 4. The T_{cr}, T_u, and θ_u of the concrete beams have been considerably improved with the use of continuous spiral NSM steel wire rope.

3.1 Ultimate Torsional Moment Carrying Capacity

The ultimate torsional moment carrying capacities of the control and strengthened beams are shown in Fig. 8. The ultimate torsional moment carrying capacity of the strengthened beams semi-linearly improved relative to the control beam. Beam SNSM113 had the maximum ultimate torsional moment (25.75 kN m), beam SNSM566 had the minimum torsional moment (12.58 kN m) and the torsional moments of all the other strengthened beams lie between the two peaks.

Fig. 5 Groove filling with epoxy.

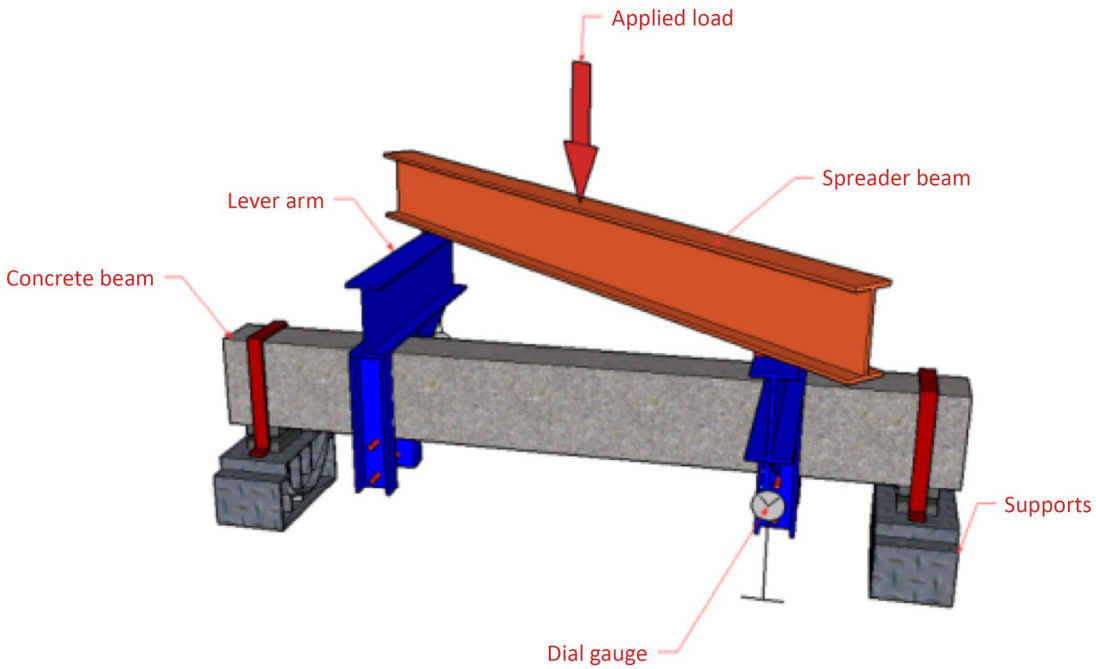

Fig. 6 Schematic of the test setup for applying combined torsion and bending.

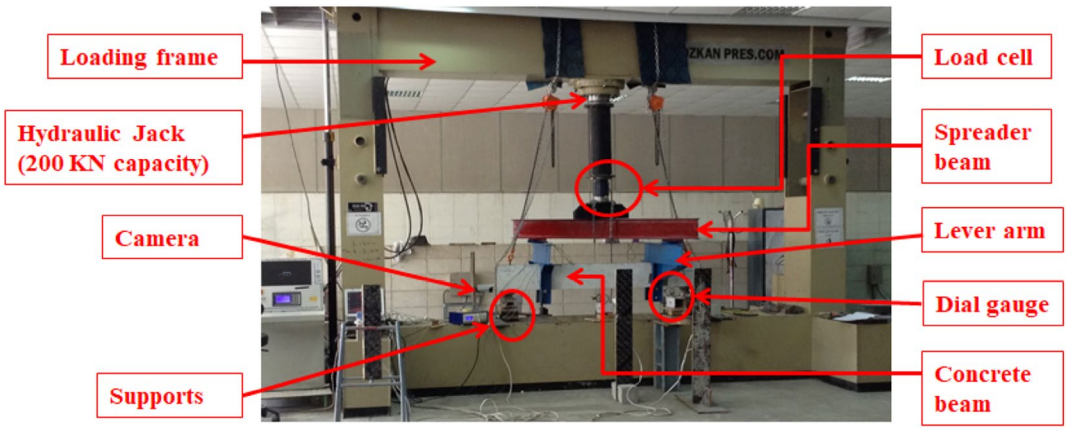

Fig. 7 Test setup with the loading frame.

Table 4 Experimental results of the tested beams.

Beam code	Str. Tech.	*f'c* MPa	$\frac{\rho_{SNSM}}{10000}$	T_{cr} KN m	%Incr.T_{cr}	T_u KN m	%Incr.T_u	θ_u deg./m	%Incr. θ_u
Control	Un-str.	48	0	4.50	0	10.75	0	4.77	0
SNSM113	Spiral NSM Steel wire rope		86	14.75	228	25.75	140	9.76	105
SNSM141			69	7.50	67	22.75	112	12.86	170
SNSM188			52	7.00	56	17.90	67	7.97	67
SNSM283			35	7.00	56	15.78	47	6.14	29
SNSM566			17	6.25	39	12.58	17	5.78	21

Str. Tech. strengthening technique, *%Incr.*T_{cr} percentage increase in cracking torque, *%Incr.*T_u percentage increase in ultimate torque, *%dec.* θ_u percentage decrease in ultimate twist angle, *Un-str.* unstrengthened.

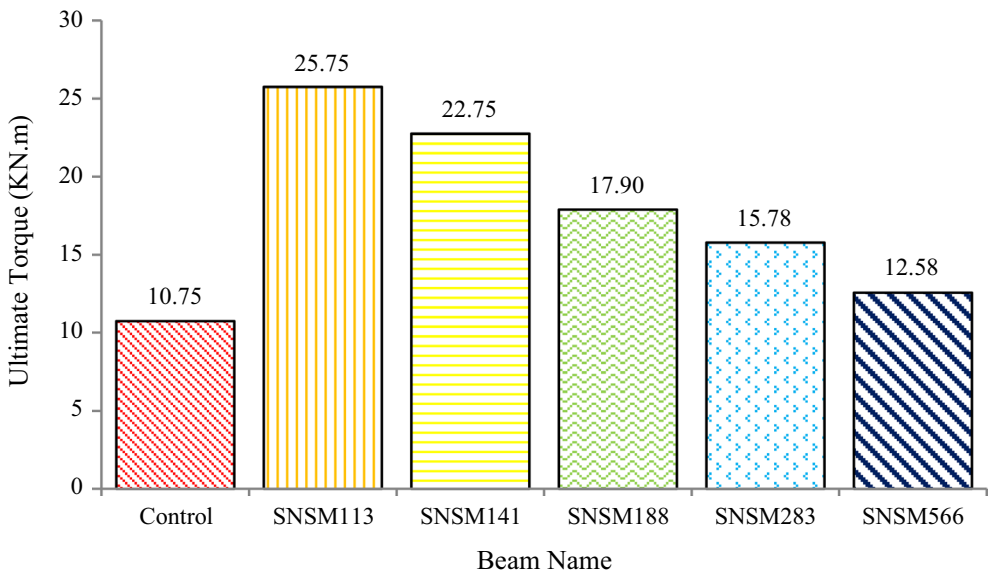

Fig. 8 Ultimate torsional moment carrying capacities of the beam specimens.

The spiral NSM steel wire rope reinforcement ratios for the strengthened beams and the corresponding increase in their ultimate torsional moment (T_u) with respect to the control beam are shown in Fig. 9. Beam SNSM113 had the maximum spiral NSM steel wire rope reinforcement ratio of 0.86% and the maximum increase in ultimate torsional moment of 140% relative to the control beam. By contrast, beam SNSM566 had the minimum spiral NSM steel wire rope reinforcement ratio of 0.17% and the minimum increase in ultimate torsional moment of 17%. For beams SNSM141, SNSM188 and SNSM283, the values of spiral NSM steel wire rope reinforcement ratios were 0.69%, 0.52% and 0.35%, respectively. The corresponding increases in their ultimate torsional moment (T_u) with respect to the control beam were 112%, 67% and 47%.

3.2 Influence of Spiral NSM Steel Wire Rope on Torsional Strength

3.2.1 Influence of Spiral NSM Steel Wire Rope Reinforcement Ratio on Torsional Strength

The influence of continuous spiral NSM steel wire rope reinforcement ratio on the torsional strength of the strengthened beams and the corresponding increase in their ultimate torsional moments (T_u) to the control beam is shown in Fig. 10. The increase in spiral NSM steel wire rope reinforcement ratios also increased the ultimate torsional strength in a linear form. The values slightly changed for beam SNSM188. Specifically, the values were below the line that represents the enhancement in the ultimate torsional moment concerning the spiral NSM steel wire rope reinforcement ratio.

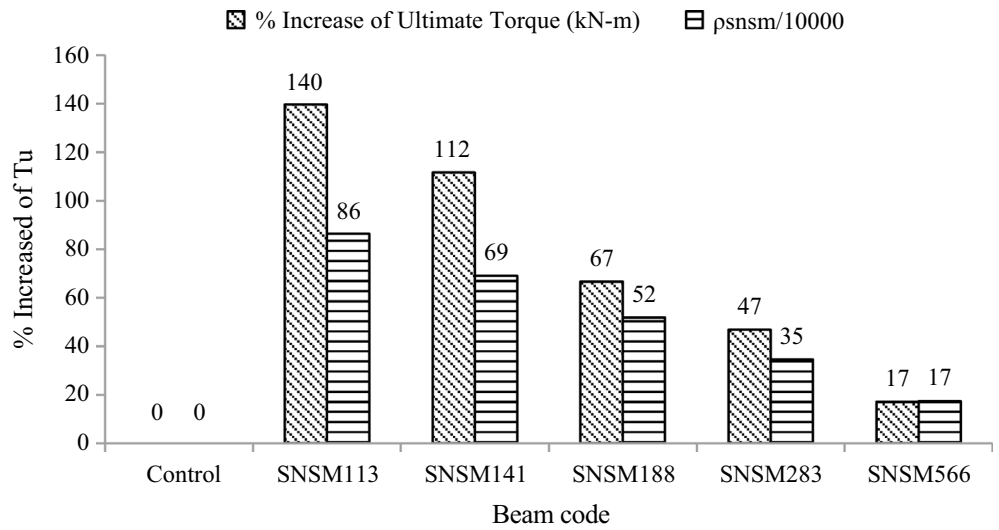

Fig. 9 Spiral NSM steel wire rope ratios and percentage improvements in the ultimate torque of the beam specimens.

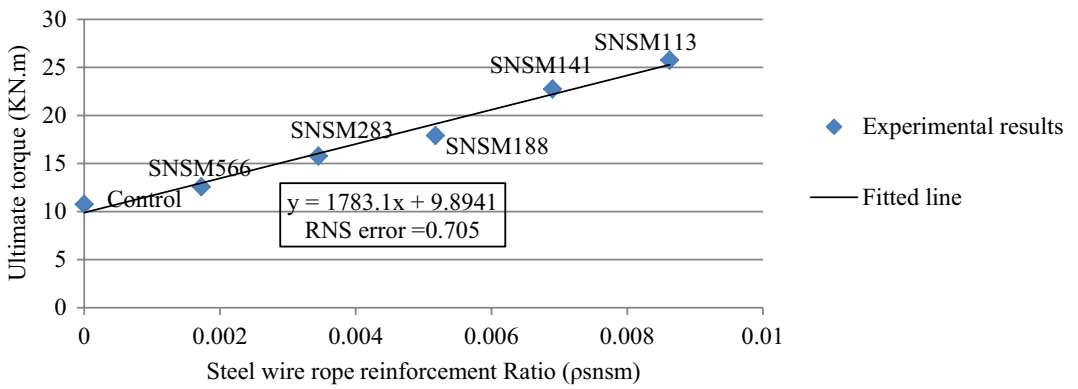

Fig. 10 Influence of NSM steel reinforcement ratio on the torsional strength of concrete beams.

3.2.2 Influence of c/c Spacing of Spiral NSM Steel Wire Rope on Torsional Strength

The effect of the c/c spacing of spiral NSM steel wire rope on the ultimate torsional moment (T_u) of strengthened beams is shown in Fig. 11. As the c/c spacing of the continuous spiral NSM steel wire ropes decreased, the ultimate torsional moment (T_u) enhanced approximately in a linear form.

3.3 Torque–Twist Comparison

The torque–twist relation of all beams is illustrated in Fig. 12. The ultimate torsional moment (T_u) and the post-cracking torsional response of all the strengthened beams indicated that the continuous spiral NSM steel wire rope reinforcement strongly affected the torsional capacity and the overall behaviour. The increase in the amount of the steel wire rope provided caused significant enhancement in the torsional carrying capacity and ductility of all strengthened beams. The control beam had lower carrying capacity of torque and higher twist angle values than the beams strengthened by spiral NSM steel wire rope under the same load. Strengthened beam SNSM behaved the same as the control beam with different changes at the latest stage of the torque–twist curves. Furthermore, the torque–twist angle tendency of all beams did not show any significant changes before the cracking. Throughout the post-cracking stage, all curves tried to show a consistent slope to reach the ultimate torque of beams due to the stirrup or the external spiral NSM steel wire rope reinforcement that resists the torque loaded on the beams. Consequently, the torsional rigidity of the beams increased and the loading stopped after reaching the ultimate torque. Beam SNSM113 was the most ductile (high torque carrying capacity and less angle of twist) amongst all the tested beams and was followed by SNSM141, SNSM188 and SNSM283.

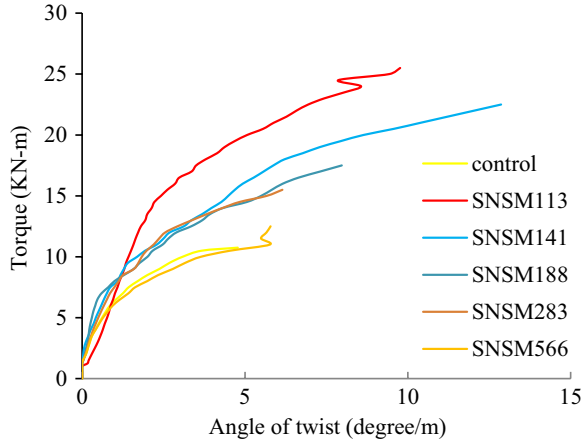

Fig. 12 Torque versus twist angle of each concrete beam.

3.4 Ultimate Bending Moment and Ultimate Mid-span Deflection Analysis

The results of ultimate bending moment and ultimate mid-span deflection for control and strengthened beams are listed in Table 5. It can be seen that the ultimate bending moment and ultimate mid-span deflection of strengthened beams increases linearly according to the continuous spiral NSM steel wire rope reinforcement ratios (ρ_{SNSM}). Among all, SNSM113 has maximum ρ_{SNSM} (0.0086), its enhancement percentage in ultimate bending moment and mid-span deflection ratio with respect to control beam is 140% and 3.17, respectively. While, SNSM566 has minimum ρ_{SNSM} (0.0017), its enhancement percentage in ultimate bending moment (M_u) and mid-span deflection ratio with respect to control beam is 17% and 1.03, respectively. The percentage of enhancement in ultimate bending moment (M_u) for beams SNSM141, SNSM188, and SNSM 283 with ρ_{SNSM} of 0.0069, 0.0052, and 0.0035 are 112%, 67%, and 47%, respectively. The

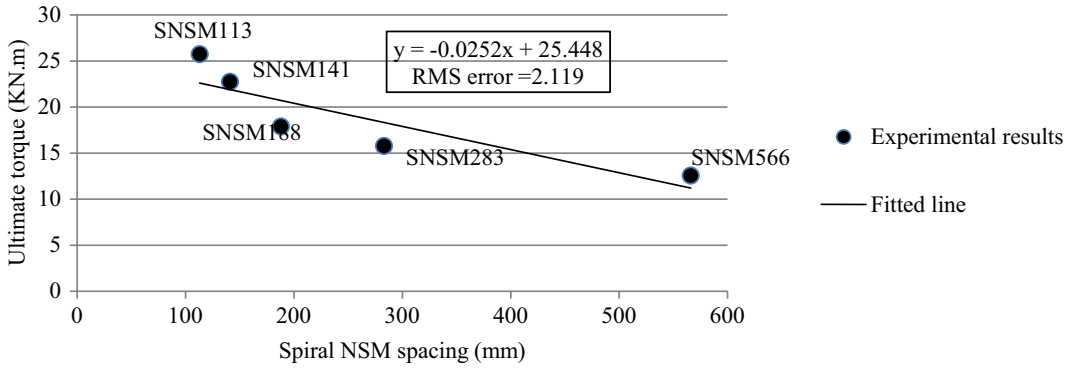

Fig. 11 Influence of spiral NSM spacing on ultimate torsional moment.

Table 5 Bending moment and mid-span deflection.

Beam code	Ultimate bending moment (KN m)	% increase of ultimate bending moment (kN m)	Mid-span deflection (mm)	% increase of mid-span deflection (mm)	Deflection ratio
Control	8.6	0	2.97	0	1.00
SNSM113	20.6	140	9.41	217	3.17
SNSM141	18.2	112	9.02	204	3.04
SNSM188	14.32	67	6.88	132	2.32
SNSM283	12.62	47	5.63	90	1.90
SNSM566	10.06	17	3.05	3	1.03

mid-span deflection ratio with respect to control beam for beams SNSM141, SNSM188, and SNSM 283 with ρ_{SNSM} of 0.0069, 0.0052, and 0.0035 are 3.04, 2.32, and 1.90, respectively.

3.5 Contribution of Continuous Spiral NSM Steel Wire Rope to the Post-elastic Response

For a complete knowledge and evaluation of the continuous spiral NSM steel wire rope contribution on the response and for comparison reasons of test results in terms of torsional ductility indices, the following torsional ductility indices are introduced, which are used by (Chalioris and Karayannis 2009):

$$\mu_T = \frac{\vartheta_{Tmax}}{\vartheta_{Tcr}} \tag{2}$$

$$\mu_{T85max} = \frac{\vartheta_{85Tmax}}{\vartheta_{Tmax}} \tag{3}$$

$$\mu_{T85cr} = \frac{\vartheta_{85Tmax}}{\vartheta_{Tcr}} \tag{4}$$

ϑ_{Tmax} is the rotation at the maximum torsional moment, degree/m; ϑ_{85Tmax} is the rotation at the point of 85% of the maximum torsional moment, assumed as the end of the reliable response range, degree/m

Values of the above mentioned torsional ductility indices for the tested beams are listed in Table 6. The results showed that the increase of continuous spiral NSM steel wire rope ratio results in a significant improvement of the post-elastic behaviour of the beams.

3.6 Crack Pattern and Failure Modes

The failure modes of the control and strengthened beams are shown in Fig. 13. The torsional moment forced all the tested beams to fail. The number of cracks in the strengthened beams was larger than that in the control beam; thus, the former beams had higher tensile stress than the latter beam. The development of flexural cracks at the mid-point length of one or both of the vertical faces of the beam was observed in the control beam. Torsional tension cracks were formed and propagated in some kind of spiral pattern. The continuous spiral NSM steel wire rope strengthened beams demonstrated different failure modes and mechanisms since steel wire rope delay crack growth and propagation in strengthened beams. For low spiral NSM steel wire rope reinforcement ratios this improvement in first crack strength is of minor important. As the load increased, the cracks expanded gradually, the two arms rotating in the opposite directions relative to each other around the longitudinal axis of the beams. Most of the concrete cracks in the strengthened beams were located between the spiral NSM wire ropes through the concrete surfaces. In addition, steel wire rope failure in specimen SNSM113 was observed from the edge of the central portion of the beam specimen, and the RC beam suddenly failed. For SNSM141, the first crack appeared at the centre of the test region and in both sides of the specimen. Such cracks

Table 6 Torsional ductility indices.

Beam code name	ϑ_{Tcr} (deg./m)	ϑ_{Tmax} (deg./m)	ϑ_{85Tmax} (deg./m)	μ_T	μ_{T85max}	μ_{T85cr}
Control	0.5	4.77	2.37	9.54	0.50	4.74
SNSM113	2.32	9.76	6.27	4.21	0.64	2.70
SNSM141	2.21	9.5	7.29	4.30	0.77	3.30
SNSM188	1.8	7.97	5.5	4.43	0.69	3.06
SNSM283	1.3	6.14	5.05	4.72	0.82	3.88
SNSM566	1.05	5.78	4.54	5.50	0.79	4.32

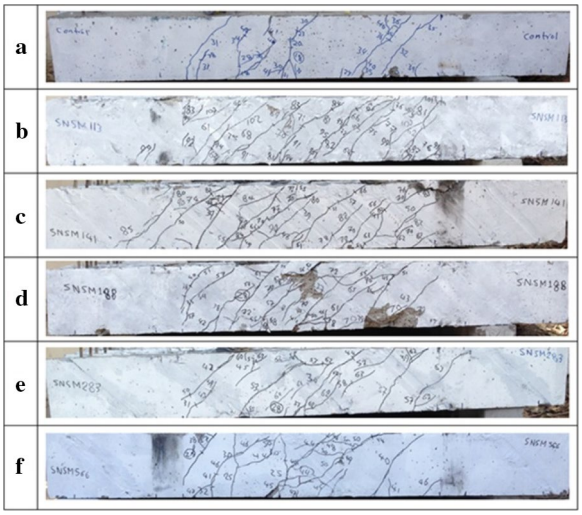

Fig. 13 Failure modes of specimens under combined torsion and bending: **a** control specimen, **b** SNSM113, **c** SNSM141, **d** SNSM188, **e** SNSM283 and **f** SNSM566.

propagated and distributed in a spiral pattern throughout the central part of the test area, and the widening of the major crack in the middle of the test region resulted in a failure in that region.

By increasing the spacing between spirals NSM steel wire ropes the number of cracks decreased. The failure modes of beams SNSM113, SNSM141, SNSM188 and SNSM283 were the same. In particular, they firstly experienced sudden failure due to reaching the ultimate load of steel wire rope and then crashing of concrete. However, each beam had a different number of spiral cracks and spreading through the test region.

In SNSM566, most of the cracks concentrated at the centre of the test region, and failure occurred due to crashing of the concrete at that region.

4 Analytical Analysis

The overall torsional strength of the continuous spiral NSM steel wire rope strengthened beams can be determined using the design codes by the principle of superposition of the spiral NSM steel wire rope and conventional steel stirrups.

T_u of the spiral NSM-strengthened tested beams can be calculated by Eq. 5 as follows by adding the contributions of the spiral NSM steel wire rope and the RC beam:

$$T_u = T_{u,RC} + T_{u,SNSM}. \tag{5}$$

$T_{u,RC}$ is calculated as follows following the recommendations of (ACI 318 M-14 2014):

$$T_{u,RC} = \frac{2(0.85) \cdot A_o \cdot A_t \cdot f_{yv}}{S} \cot\theta. \tag{6}$$

The softened space truss theory can be adopted for the problem of torsion in RC beams with main bars and stirrups (vertical and spiral). The applied torsional moment T is considered to be equal to the internal resisting torque resulting from the shear flow q as shown in Fig. 14. Further, based on the stresses equilibrium, the following relationships are derived for the calculation of the torsional components T_T and T_L, due to the locking spiral steel and longitudinal reinforcement (bars and spiral stirrups) (Chalioris and Karayannis 2013):

$$T_{u,SNSM} = T_{T,SNSM} + T_{L,SNSM} \tag{7}$$

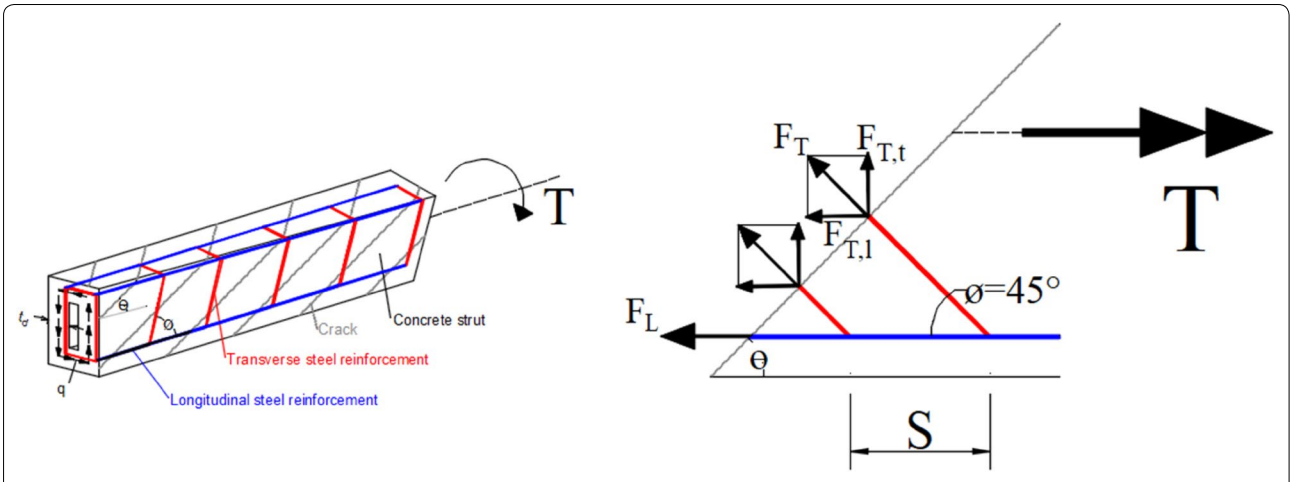

Fig. 14 Simplified torsional analysis based on the space truss theory.

$$T_{T,SNSM} = \frac{2.A_{o,SNSM} \cdot A_{ss} \cdot f_{st,SNSM} \cdot SinØ}{S_{SNSM}} Cot\theta. \quad (8)$$

$$T_{L,SNSM} = \frac{2\left(A_o \cdot A_{sl} \cdot f_{sl} + A_{o,SNSM} \cdot A_{ss} \cdot f_{st,SNSM} \cdot \cos Ø\right)}{P_{SS}} \tan\theta \quad (9)$$

For calculating actual inclination of the diagonal compression struts (cracking angle), we can use Eq. 10 for unstrengthened (Control) beam and Eq. 11 for continuous spiral NSM strengthened beams.

$$\tan\theta = \sqrt{\frac{A_t \cdot f_{st} \cdot P_o}{A_{sl} \cdot f_{sl} \cdot S}} \quad (10)$$

$$\tan\theta = \sqrt{\frac{A_t f_{st} P_o + A_{ss} f_{st,SNSM} \sin Ø P_{ss}}{\left(A_{sl} f_{sl} + A_{ss} f_{st,SNSM} \cos Ø\right) S/\sin Ø}} \quad (11)$$

Table 7 Comparison of the experimental and analytical ultimate torsional moments.

Beam name code	Ultimate torsional moment T_u (KN m)		$T_{u,Exp.}/T_{u,An.}$
	Experimental	Analytical	
Control	10.75	11.34	0.95
SNSM113	25.75	26.71	0.96
SNSM141	22.75	24.80	0.92
SNSM188	17.90	15.37	1.16
SNSM283	15.78	16.81	0.94
SNSM566	12.58	14.51	0.87

Table 7 and Fig. 15 compare the experimental and predicted results for torsional capacity by using the (ACI 318 M-14 2014) design model equations and equations from (Chalioris and Karayannis 2013). The torsional capacity for the control beam was overestimated by 5% because the model was established on the basis of space truss theory, which ignores the contribution of the dowel action of longitudinal reinforcement which was took into consideration in this study. The strengthened RC beams SNSM113, SNSM141, SNSM283 and SNSM566 were overestimated by 4%, 8%, 6% and 13%, respectively, because of the mentioned reasons for control beam. The strengthened RC beam SNSM188 was underestimated by 16%.

5 Conclusions

Apart from the shear and flexural strength of RC beams, this study also examines the torsional behaviour of RC beams that were strengthened with various continuous spiral NSM steel wire rope configurations under the

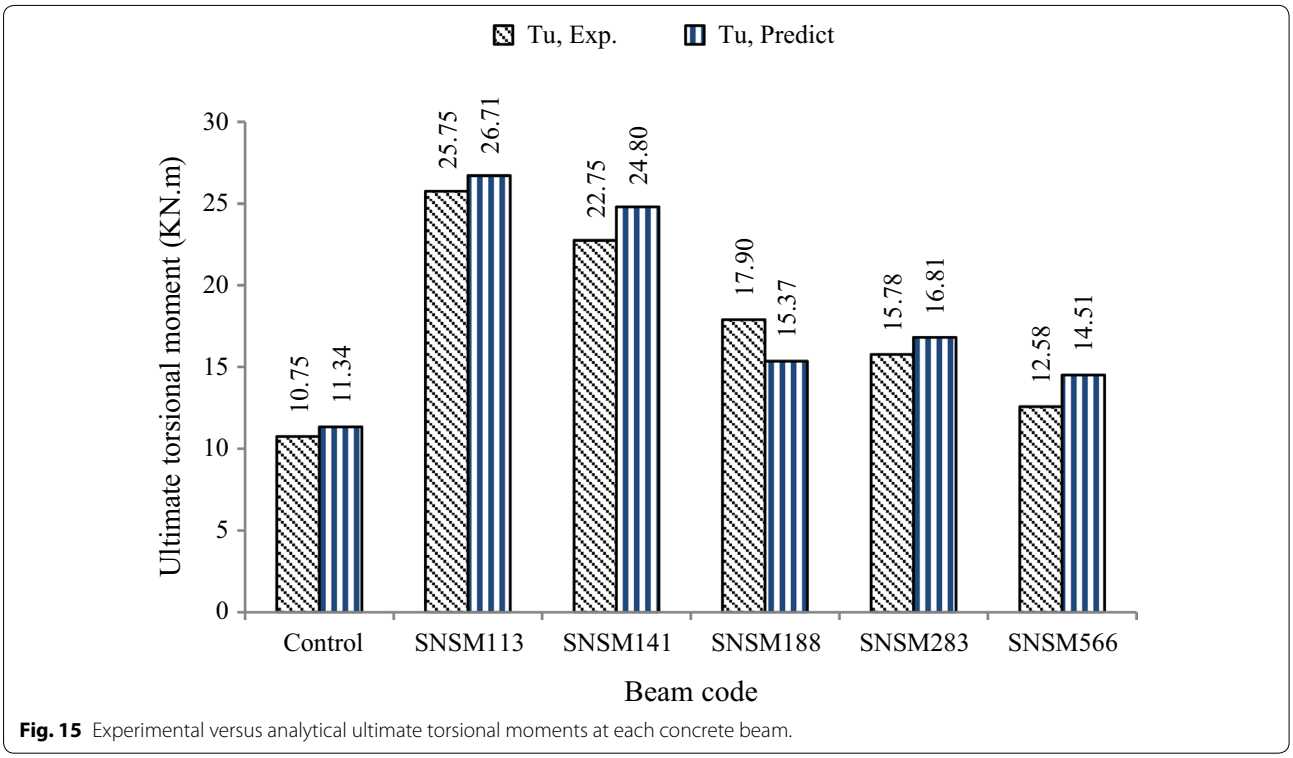

Fig. 15 Experimental versus analytical ultimate torsional moments at each concrete beam.

simultaneous effect of torsion and bending. From the experimental results the following conclusions can be drawn:

- All beams strengthened by the spiral NSM steel wire rope showed higher torsional resistance than the control beam regardless of the spiral NSM steel wire rope spacing.
- Spiral configuration is the effective technique because the inclined steel wire ropes were in tension up to failure.
- The SNSM113 test beam with an Ø8 mm spiral NSM steel wire rope at 113 mm c/c spacing showed the maximum (140%) increment in ultimate torque compared with the control beam. By contrast, the SNSM566 beam with an Ø8 mm spiral NSM steel wire rope at 566 mm c/c spacing showed the minimum (17%) increment in ultimate torque compared with the control beam.
- The SNSM113 test beam with an Ø8 mm spiral NSM steel wire rope at 113 mm c/c spacing showed the maximum (226%) increment in cracking torque compared with the control beam. On the contrary, the SNSM566 beam with an Ø8 mm spiral NSM steel wire rope at 566 mm c/c spacing showed the minimum (39%) increment in cracking torque compared with the control beam.
- The ductility of the strengthened beams improved and such increment was significant for some spiral NSM steel wire rope spacing.
- The percentage increase in T_u proportionally increased with the increase in the spiral NSM steel wire rope ratio.
- The cracks in the strengthened specimens spread widely throughout the testing area relative to the singular cracks generated in the control one.
- The concrete beam failure was delayed for the beams strengthened with spiral NSM steel wire rope. However, such failure occurred in the unstrengthened region space between the spirals NSM steel wire ropes.
- The ultimate torsional and bending moments increased by reducing the spacing between the spirals NSM steel wire ropes (i.e. increasing the spiral NSM steel wire rope ratios).
- The predicted ultimate torsional moment of the RC beams strengthened by the continuous spiral NSM steel wire rope showed a good agreement with the experimental results.

Abbreviations

Acronyms

NSM: near surface mounted; SNSM: spiral near surface mounted; FRP: fibre-reinforced polymer; CFRP: carbon-fibre-reinforced polymer; RC: reinforced concrete; EBR: externally bonded reinforcement.

List of Symbols

A_c: gross area of the concrete cross-section, mm^2; A_o: cross-sectional area bounded by the centre line of the shear flow, mm^2; $A_{o,SNSM}$: cross-sectional area bounded by the centre line of the shear flow (spiral NSM steel wire rope), mm^2; A_{sl}: area of internal main reinforcement, mm^2; A_{ss}: area of the NSM steel wire rope reinforcement, mm^2; A_t: area of transversal steel reinforcement (spiral or stirrup), mm^2; $A_{t,SNSM}$: area of one legged steel stirrup or NSM steel wire rope reinforcement, mm^2; f'_c: concrete compressive strength, MPa; f_{sl}: tensile strength of the longitudinal main steel reinforcement, MPa; $f_{st,SNSM}$: measured ultimate tensile strength of the transverse steel reinforcement (spirals), MPa; f_{yv}: yield stress of transversal steel reinforcement, MPa; P_{ss}: perimeter of the spiral NSM steel wire rope in one pitch, mm; S: horizontal c/c spacing of the internal stirrup, mm; S_{SNSM}: c/c spacing of the spiral NSM steel wire rope, mm; T_{cr}: cracking torque, kN m; $T_{L,SNSM}$: resisting longitudinal torsional component due to the spiral steel wire rope and dowel action of main reinforcement, kN m; $T_{T,SNSM}$: resisting transverse torsional component due to the spiral steel wire rope, kN m; T_u: ultimate torsional capacity of the spiral NSM-strengthened beam, kN m; $T_{u,An}$: analytical ultimate torsional moment, kN m; $T_{u,Exp}$.: experimental ultimate torsional moment, kN m; $T_{u,RC}$: ultimate torsional capacity from steel reinforcement, kN m; $T_{u,SNSM}$: ultimate torsional capacity from spiral NSM wire rope reinforcement, kN m; θ: inclination of the diagonal compression struts (cracking angle), deg; θ_u: ultimate twist angle, deg; ϑ_{85Tmax}: the rotation at the point of 85% of the maximum torsional moment, assumed as the end of the reliable response range, deg; ϑ_{Tmax}: the rotation at the maximum torsional moment, deg; ϑ_{cr}: first cracking twist angle, deg; Ø: angle between spiral NSM steel wire rope reinforcement and the longitudinal axis of the beam (Ø = 45°); ρ_{snsm}: NSM spiral steel wire rope reinforcement ratio, mm^2/mm^2; μ: reinforced concrete beam torsional ductility factor.

Acknowledgements

The authors acknowledge the support of Salahaddin University in Erbil and Sulaimani Polytechnic University in Sulaymaniyah.

Authors' contributions

Corresponding author NHA as a researcher and Ph.D. student did the experimental, theoretical and writing the manuscript. ADM role as supervisor. Both authors read and approved the final manuscript.

Funding

The authors declare that no funding was received.

Availability of data and materials

All data is provided in full in the results section of this paper.

Competing interests

The authors declare that they have no competing interests.

Author details

[1] Halabja Technical College of Applied Sciences, Sulaimani Polytechnic University, Sulaymaniyah, Iraq. [2] Department of Civil Engineering, Salahaddin University, Erbil, Iraq.

Received: 27 June 2019 Accepted: 16 December 2019
Published online: 21 February 2020

References

ACI 318 M–14. (2014). *Building code requirements for structural concrete*. Farmington Hills: American Concrete Institute.

ACI 440.2R-08. (2008). *Guide for the design and construction of externally bonded FRP systems for strengthening concrete structures*. Farmington Hills: American Concrete Institute.

Al-Bayati, G., Al-Mahaidi, R., Hashemi, M. J., & Kalfat, R. (2018). Torsional strengthening of RC beams using NSM CFRP rope and innovative adhesives. *Composite Structures, 187,* 190–202.

Al-Bayati, G., Al-Mahaidi, R., & Kalfat, R. (2016). Experimental investigation into the use of NSM FRP to increase the torsional resistance of RC beams using epoxy resins and cement-based adhesives. *Construction and Building Materials, 124,* 1153–1164.

Al-Mahmoud, F., Castel, A., François, R., & Tourneur, C. (2010). RC beams strengthened with NSM CFRP rods and modeling of peeling-off failure. *Composite Structures, 92,* 1920–1930.

Almassri, B. (2015). *Strengthening of corroded reinforced concrete (RC) beams with near surface mounted (NSM) technique using carbon fiber polymer (CFRP) rods; an experimental and finite element (FE) modelling study*. Toulouse: INSA.

Almusallam, T. H., Elsanadedy, H. M., Al-salloum, Y. A., & Alsayed, S. H. (2013). Experimental and numerical investigation for the flexural strengthening of RC beams using near-surface mounted steel or GFRP bars. *Construction and Building Materials, 40,* 145–161.

Askandar, N., & Mahmood, A. (2019). Comparative investigation on torsional behaviour of RC beam strengthened with CFRP fabric wrapping and near-surface mounted (NSM) steel bar. *Advances in Civil Engineering, 2019,* 15.

ASTM A370–10. (2010). *Standard test methods and definitions for mechanical testing of steel products*. West Conshohocken: ASTM International.

Barros, J., Dias, S. & Fortes, A. 2005. Near surface mounted technique for the flexural and shear strengthening of concrete beams. In *International Conference on Concrete for Structures* Coimbra, Portugal: University of Coimbra.

Breveglieri, M., Aprile, A., & Barros, J. A. (2014). Shear strengthening of reinforced concrete beams strengthened using embedded through section steel bars. *Engineering Structures, 81,* 76–87.

Chalioris, C. E., & Bantilas, K. E. (2017). Shear strength of reinforced concrete beam-column joints with crossed inclined bars. *Engineering Structures, 140,* 241–255.

Chalioris, C. E., Favvata, M. J., & Karayannis, C. G. (2008). Reinforced concrete beam–column joints with crossed inclined bars under cyclic deformations. *Earthquake engineering structural dynamics, 37,* 881–897.

Chalioris, C. E., & Karayannis, C. G. (2009). Effectiveness of the use of steel fibres on the torsional behaviour of flanged concrete beams. *Cement & Concrete Composites, 31,* 331–341.

Chalioris, C. E., & Karayannis, C. G. (2013). Experimental investigation of RC beams with rectangular spiral reinforcement in torsion. *Engineering Structures, 56,* 286–297.

Chalioris, C., Kosmidou, P.-M., & Papadopoulos, N. (2018). Investigation of a new strengthening technique for RC deep beams using carbon FRP ropes as transverse reinforcements. *Fibers, 6,* 52.

De Lorenzis, L., & Nanni, A. (2001). Shear strengthening of reinforced concrete beams with near-surface mounted fiber-reinforced polymer rods. *ACI Structural Journal, 98,* 60–68.

De Lorenzis, L., & Teng, J. G. (2007). Near-surface mounted FRP reinforcement: An emerging technique for strengthening structures. *Composites Part B Engineering, 38,* 119–143.

El-Gamal, S., Al-Nuaimi, A., Al-Saidy, A. & Al-Lawati, A. 2014. Flexural strengthening of RC beams using near surface mounted fibre reinforced polymers. In *Brunei International Conference on Engineering and Technology.* Brunei Darussalam.

El-Hacha, R., & Gaafar, M. (2011). Flexural strengthening of reinforced concrete beams using prestressed, near-surfacemounted CFRP bars. *PCI Journal, 56,* 134–151.

Franco, N., Biscaia, H., & Chastre, C. (2018). Experimental and numerical analyses of flexurally-strengthened concrete T-beams with stainless steel. *Engineering Structures, 172,* 981–996.

Ghanim, A. & Al-abbas, B. 2018. Experimental Study on the Flexural Strengthening of Reinforced Concrete Beams Using NSM CFRP Bars. In *5th national and 1st international conference on modern materials and structures in civil engineering, At Amirkabir University of Technology.* Tehran-Iran.

Gopinath, S., Murthy, A. R., & Patrawala, H. (2016). Near surface mounted strengthening of RC beams using basalt fiber reinforced polymer bars. *Construction and Building Materials, 111,* 1–8.

Haryanto, Y., Gan, B., Widyaningrum, A., Wariyatno, N. G., & Fadli, A. (2018). On the performance of steel wire rope as the external strengthening of RC beams with different end-anchor types. *Jurnal Teknologi, 80,* 145–154.

Hindi, R. A., & Browning, B. J. (2011). Torsionally loaded circular concrete members confined with spirals. *ACI Structural Journal, 108,* 139–147.

Hong, K., Lee, S., Yeon, Y., & Jung, K. (2018). Flexural response of reinforced concrete beams strengthened with near-surface-mounted Fe-based shape-memory alloy strips. *International Journal of Concrete Structures and Materials, 12,* 1–13.

Hosen, M., Alengaram, U. J., Jumaat, M. Z., Sulong, N., & Darain, K. (2017). Glass Fiber Reinforced Polymer (GFRP) bars for enhancing the flexural performance of RC beams using side-NSM technique. *Polymers, 9,* 180.

Hosen, M., Jumaat, M., Alengaram, U., Islam, A., & Bin Hashim, H. (2016). Near surface mounted composites for flexural strengthening of reinforced concrete beams. *Polymers, 8,* 67.

Hosen, M. A., Jumaat, M. Z., Darain, K. M. U., Obaydullah, M. & Islam, A. S. 2014. Flexural Strengthening of RC Beams with NSM Steel Bars. In *Proceedings of the International Conference on Food, Agriculture and Biology (FAB-2014)*.

Kammona, H. H., & Al-Issawi, A. S. H. (2018). Estimation of maximum shear capacity of RC deep beams strengthened by NSM steel bars. *Journal of University of Babylon, 26,* 13–22.

Karayannis, C. G., & Chalioris, C. E. (2013). Shear tests of reinforced concrete beams with continuous rectangular spiral reinforcement. *Construction and Building Materials, 46,* 86–97.

Karayannis, C., Chalioris, C., Mavroeidis, P. D. 2005. Shear capacity of RC rectangular beams with continuous spiral transversal reinforcement. *CWIT Transactions on Modelling Simulation*, *41*, 379–386.

Kaya, E., Kütan, C., Sheikh, S., & İlki, A. (2016). Flexural retrofit of support regions of reinforced concrete beams with anchored frp ropes using nsm and ets methods under reversed cyclic loading. *Journal of Composites for Construction, 21,* 04016072.

Kim, S. Y., Yang, K. H., Byun, H. Y., & Ashour, A. F. (2007). Tests of reinforced concrete beams strengthened with wire rope units. *Engineering Structures, 29,* 2711–2722.

Kishi, N., Mikami, H., Kurihashi, Y. & Sawada, S. 2005. Flexural behaviour of RC beams reinforced with NSM AFRP rods. In *Proceedings of the International Symposium on Bond Behaviour of FRP in structures* (*BBFS 2005*). pp. 337–342.

Li, X., Wu, G., Popal, M. S., & Jiang, J. (2018). Experimental and numerical study of hollow core slabs strengthened with mounted steel bars and prestressed steel wire ropes. *Construction and Building Materials, 188,* 456–469.

Mofidi, A., Chaallal, O., Cheng, L., & Shao, Y. (2015). Investigation of near surface–mounted method for shear rehabilitation of reinforced concrete beams using fiber reinforced–polymer composites. *Journal of Composites for Construction, 20,* 04015048.

Noroozieh, E., & Mansouri, A. (2019). Lateral strength and ductility of reinforced concrete columns strengthened with NSM FRP rebars and FRP jacket. *International Journal of Advanced Structural Engineering (IJASE), 11,* 195–209.

Rahal, K. N., & Rumaih, H. A. (2011). Tests on reinforced concrete beams strengthened in shear using near surface mounted CFRP and steel bars. *Engineering Structures, 33,* 53–62.

Ramezanpour, M., Morshed, R., & Eslami, A. (2018). Experimental investigation on optimal shear strengthening of RC beams using NSM GFRP bars. *Structural Engineering Mechanics, 67,* 45–52.

Saha, P., & Meesaraganda, L. V. (2019). Experimental investigation of reinforced SCC beam-column joint with rectangular spiral reinforcement under cyclic loading. *Construction and Building Materials, 201,* 171–185.

Seo, S.-Y., Choi, K.-B., Kwon, Y.-S., & Lee, K.-S. (2016). Flexural strength of RC beam strengthened by partially De-bonded near surface-mounted FRP strip. *International Journal of Concrete Structures and Materials, 10,* 149–161.

Sharaky, I., Reda, R., Ghanem, M., Seleem, M., & Sallam, H. (2017). Experimental and numerical study of RC beams strengthened with bottom and side NSM GFRP bars having different end conditions. *Construction and Building Materials, 149,* 882–903.

Sharaky, I. A., Torres, L., Comas, J., & Barris, C. (2014). Flexural response of reinforced concrete (RC) beams strengthened with near surface mounted (NSM) fibre reinforced polymer (FRP) bars. *Composite Structures, 109,* 8–22.
Shatarat, N., Katkhuda, H., Abdel-Jaber, M. T., & Alqam, M. (2016). Experimental investigation of reinforced concrete beams with spiral reinforcement in shear. *Construction and Building Materials, 125,* 585–594.
Shukri, A., Hosen, M., Muhamad, R., & Jumaat, M. (2016). Behaviour of precracked RC beams strengthened using the side-NSM technique. *Construction and Building Materials, 123,* 617–626.
Tiwary, A. K. & Mohan, M. 2015. Strengthening of exterior beam column joint with modified reinforcement technique. In *National conference on advances in engineering, technology & management (AETM'15)*. Sadopur, Ambala: Maharishi Markandeshwar University.
Wei, Y., & Wu, Y.-F. (2014). Compression behavior of concrete columns confined by high strength steel wire. *Construction and Building Materials, 54,* 443–453.
Wei, Y., Zhang, X., Wu, G., & Zhou, Y. (2018). Behaviour of concrete confined by both steel spirals and fiber-reinforced polymer under axial load. *Composite Structures, 192,* 577–591.
Wu, G., Dong, Z.-Q., Wu, Z.-S., & Zhang, L.-W. (2013). Performance and parametric analysis of flexural strengthening for RC beams with NSM-CFRP bars. *Journal of Composites for Construction, 18,* 04013051.
Yang, K.-H., Byun, H.-Y., & Ashour, A. F. (2009). Shear strengthening of continuous reinforced concrete T-beams using wire rope units. *Engineering Structures, 31,* 1154–1165.
Zhang, S. S., Yu, T., & Chen, G. (2017). Reinforced concrete beams strengthened in flexure with near-surface mounted (NSM) CFRP strips: Current status and research needs. *Composites Part B Engineering, 131,* 30–42.

Publisher's Note